

1 **CD150-dependent hematopoietic stem cells sensing of *Brucella***
2 **instructs myeloid commitment**

3
4 Hysenaj Lisiena^{1,2#}, De Laval Bérengère^{1#}, Arce-Gorvel Vilma¹, Bosilkovski Mile³, Gonzalez
5 Gabriela¹, Debroas Guillaume¹, Sieweke Michael^{1,4§}, Sarrazin Sandrine^{1§*} and Gorvel Jean-
6 Pierre^{1§*}

7
8 1 : Aix Marseille University, CNRS, INSERM, CIML, 13009 Marseille, France

9 2 : Department of Anatomy, University of California, San Francisco, USA

10 3 : University Clinic for Infectious Diseases and Febrile Conditions, Skopje, Republic of North
11 Macedonia,

12 4 : Center for Regenerative Therapies Dresden (CRTD), Technische Universität Dresden, 01307
13 Dresden, Germany

14
15 # : co-first author

16 § : co-last author

17 *Corresponding authors:

18 Jean-Pierre Gorvel, gorvel@ciml.univ-mrs.fr, Orcid: <https://orcid.org/0000-0002-2829-9804>
19 Centre d'Immunologie de Marseille-Luminy, Marseille, France

20
21 Sandrine Sarrazin, sarrazin@ciml.univ-mrs.fr, Orcid: <https://orcid.org/0000-0001-6435-0913>
22 Centre d'Immunologie de Marseille-Luminy, Marseille, France

23
24 **SUMMARY**

25 This work provides first evidence HSC directly sense *Brucella abortus* via the bacterial outer
26 membrane protein Omp25 and the HSC surface receptor CD150, leading to functional commitment
27 of HSC to myeloid lineage and very early initiation of immune response.

28 **ABSTRACT**

29 So far, hematopoietic stem cells (HSC) are considered the source of mature immune cells, the latter
30 being the only ones capable of mounting an immune response. Recent evidence shows HSC can
31 also directly sense cytokines released upon infection/inflammation and pathogen-associated
32 molecular pattern interaction, while keeping a long-term memory of previous encountered signals.
33 Direct sensing of danger signals by HSC induces early myeloid commitment, increases myeloid
34 effector cell numbers and contributes to an efficient immune response. Here, using specific genetic
35 tools on both host and pathogen sides, we show that HSC can directly sense *B. abortus* pathogenic
36 bacteria within the bone marrow via the interaction of the cell surface protein CD150 with the
37 bacterial outer membrane protein Omp25, inducing efficient functional commitment of HSC to the
38 myeloid lineage. This is the first demonstration of a direct recognition of a live pathogen by HSC
39 via CD150, which attests of a very early contribution of HSC to immune response.

40

41 **INTRODUCTION**

42 Few pathogens are capable of colonizing the bone marrow (BM) [1-5], the niche of haematopoietic
43 stems cells (HSCs) responsible for initiating the production of myeloid progenitors and mature
44 blood-forming cells [6]. *Brucella abortus*, (Gram-negative bacterium responsible for the re-
45 emerging zoonosis of brucellosis) is able to persist for months in the BM [7]. Human brucellosis
46 patients suffer from haematological abnormalities suggesting that *Brucella* in the BM may affect
47 hematopoietic development [8]. HSCs can respond to an infection through pathogen-elicited
48 cytokines or directly via pathogen recognition receptors (PRR) [9, 10]. CD150 is a key marker of
49 long term HSC (LT-HSCs) [11] and a microbial sensor in macrophages [12] and dendritic cells
50 [13]. Here, we show that HSCs within the BM directly sense the outer membrane protein Omp25 of
51 live *Brucella* through the CD150 receptor. Our *in vivo* and *ex vivo* data demonstrate that *B. abortus*
52 modulates hematopoiesis by transiently augmenting the production of myeloid cells via CD150.
53 This is the first demonstration of a direct recognition of a pathogen by HSCs via CD150.

54 RESULTS

55 To investigate the consequences of BM infection by a pathogen known to persist for extended
56 periods of time in the hematopoietic niche, we used *Brucella abortus*. We previously demonstrated
57 that this pathogenic bacterium persists for months in murine BM [7]. We began by evaluating if
58 bacteria present in the BM at 8 days post-infection (acute phase of infection) and at 30 days post-
59 infection (chronic phase of infection) are still virulent. For this, we transplanted BM cells of
60 infected mice at those time point into recipient mice (Fig. 1a). Spleen (the natural reservoir for *B.*
61 *abortus*) and BM cells were harvested eight weeks after transplantation, and bacterial colony
62 forming units (CFU) were enumerated (Fig.1b). The equivalently high number of bacteria in spleen
63 and bone marrow at 8 weeks post-transplantation shows that the BM hematopoietic environment is
64 permissive for stable infection and replication of *Brucella*.

65
66 To further investigate the consequences of BM infection by *B. abortus* on hematopoietic stem cell
67 biology, we analysed the distribution of the hematopoietic stem and progenitor cell compartment
68 (HSPC) by flow cytometry. Absolute numbers of total BM cells or lineage negative progenitors
69 (Lin^-) were not affected by *B. abortus* infection (Supplementary Fig. 1a, b). However, *Brucella*
70 infection induced major phenotypic cell surface marker changes in the HSPC compartment (Fig. 1c,
71 d and Supplementary Fig. 1c for gating strategy), similar to those observed after challenges with
72 PAMPs or attenuated vaccines [10, 14-16]. HSPC (LSK: Lin^- , Sca^+ , cKit^+) expansion was observed
73 at the onset of infection (Day 2 p.i., Fig. 1c, d) and was even more pronounced during the acute
74 phase of infection (Day 8 p.i., Fig. 1c, d). LSK expansion was mainly due to the significant increase
75 of CD48^+ multipotent progenitors (LSK CD48^+) and, to a lesser extent, the increase of short term
76 HSC (ST-HSC: LSK, CD34^- , CD135^- , CD48^- , CD150^-). In addition, the long-term HSC population
77 (LT-HSC: LSK, CD34^- , CD135^- , CD48^- , CD150^+) slightly decreased (Fig. 1c, d). Overall, these
78 data suggest that the presence of *Brucella* in the BM perturbs HSPC homeostasis and leads to an
79 increased output of early multipotent progenitors.

80

81 Infection and inflammation have been shown to release signals, such as cytokines, that are able to
82 induce the differentiation of HSC towards the myeloid lineage as evidenced by early up-regulation
83 of the myeloid master regulator PU.1 [17-20]. To further investigate whether *B. abortus* infection
84 can induce an early commitment towards the myeloid lineage in HSC, we infected *Pu.1^{+GFP}*
85 reporter mice harbouring enhanced green fluorescent protein (GFP) knocked into the PU.1 locus
86 [21, 22] and then analysed GFP expression in HSC (LSK, CD34⁻, CD135⁻, CD48⁺) at 2 days post-
87 infection. GFP expression in HSC was used as a read-out of early HSC activation/commitment
88 during *Brucella* infection (Fig. 2a). GFP was upregulated 30 to 40% in BM HSCs of *B. abortus*-
89 infected WT mice (Fig. 2b, left panel), confirming an induction of PU.1 expression and
90 consequently a change in HSC fate after *Brucella* infection.

91
92 We then investigated the molecular mechanisms underlying the early response of HSC during
93 *Brucella* infection. HSC can directly sense microbial compounds [14, 23, 24]. The CD150 receptor,
94 known as one of the key markers of HSC [25], is also able to sense bacteria in dendritic cells and
95 macrophages directly [12]. Indeed, in vitro studies showed that OmpC and OmpF of *E. coli* and
96 *Salmonella spp.* binds to extracellular domain of CD150 [12]. Moreover, we have recently
97 demonstrated that the outer-membrane protein 25 (Omp25) of *B. abortus* is a direct ligand of the
98 extracellular domain of mouse CD150 in dendritic cells [13]. We asked whether HSC could detect
99 *Brucella* via a direct Omp25/CD150 recognition. For this purpose we generated a new *Pu.1^{+GFP}*
100 reporter mouse model lacking CD150 (*CD150^{-/-}; Pu.1^{+GFP}*). Infected *CD150^{-/-}* mice showed
101 equivalent bacterial load in both spleen and BM during the onset and acute phase of infection
102 (Supplementary Fig. 2). Moreover, infection did not affect either the total number of BM cells or
103 the number of Lin⁻ cells in *CD150^{-/-}* mice (Supplementary Fig. 1). At 2 days post-infection, BM
104 HSC from *CD150^{-/-}; Pu.1^{+GFP}* mice did not present any increase of GFP expression (Fig. 2b, right
105 panel) in contrast to what we observed in *Pu.1^{+GFP}* mice (Fig. 2b, left panel), suggesting that the
106 induction of PU.1 by *B. abortus* is mediated by CD150.

107

108 To further test whether *B. abortus* directly binds CD150, PU.1 expression in HSC was analysed
109 during infection with *B. abortus* WT and *B. abortus* lacking Omp25 (*Ba Δomp25*) in *Pu.1^{+GFP}*
110 reporter mice (Fig. 2a). The upregulation of PU.1 observed in HSC in response to *B. abortus* WT
111 infection was abolished when infected with *Ba Δomp25* (Fig. 2b left panel), while bacterial CFU
112 counts in spleen and BM were similar to those in mice infected with *B. abortus* WT (Supplementary
113 Fig. 2). These data indicate that PU.1 upregulation in HSC during the onset of infection is
114 dependent on Omp25/CD150 interaction.

115

116 To further demonstrate that the upregulation of PU.1 in HSC upon *Brucella* infection is due to the
117 direct recognition of *B. abortus* Omp25 by CD150, we isolated HSC from the BM of *Pu.1^{+GFP}*
118 mice and treated them *ex vivo* with outer membrane vesicles (OMV) [26] from either *Brucella* WT
119 or *Ba Δomp25* (Fig. 2c). At 16 h post-*ex vivo* stimulation of sorted HSC by *B. abortus* WT OMV,
120 the number of GFP-expressing HSC increased two-fold (Fig. 2d), following the same trend as *in*
121 *vivo* infection of *Pu.1^{+GFP}* reporter mice (Fig. 2b). In contrast, upregulation of GFP-expressing
122 HSC was abolished by either incubation of HSC with *Ba Δomp25* OMV (Fig. 2d) or with *B.*
123 *abortus* WT OMV in the presence of CD150 blocking peptide (Fig. 2e) or in *CD150^{-/-}* (Fig. 2d).
124 These data demonstrate that HSC can sense bacteria via a direct interaction of *Brucella* outer
125 membrane protein Omp25 with CD150. This is the first demonstration of a direct recognition of a
126 pathogen by HSC via CD150.

127

128 PU.1 upregulation in HSCs is a first sign of commitment towards the myeloid lineage [20, 27]. We
129 therefore asked if the direct interaction between HSCs and *Brucella* induces a functional
130 commitment of HSCs towards the myeloid lineage. We analysed the composition of HSC-
131 downstream progenitors at 8 days post-infection in the BM. As expected, an increase in myeloid-
132 biased MPP2/3 (*Lin⁻, Sca⁺, cKit⁺, CD48⁺, CD135⁻*) progenitors was observed in the BM of *wt* mice
133 infected with *Ba* WT but not in the BM of *wt* mice infected with *Ba Δomp25* or infected mice

134 lacking CD150 (Fig. 3a and Supplementary Fig. 1c for gating strategy). By contrast, the number of
135 lymphoid-biased MPP4 (Lin⁻, Sca⁺, cKit⁺, CD48⁺, CD135⁺) was similar in infected and non-
136 infected mice (Fig. 3b). Moreover, analysis of downstream committed progenitors revealed an
137 increase of GMP and blood myeloid cells (Fig. 3c, d and Supplementary Fig. 1c for gating
138 strategy). In addition, infection of *wt* mice by the Ba $\Delta omp25c$ complemented strain (Ba $\Delta omp25$
139 strain complemented with an Omp25-expressing plasmid) was able to rescue the increase of
140 myeloid MPP2-3 and GMP demonstrating a direct role of Omp25 in controlling the increase of
141 myeloid commitment via CD150 (Fig. 3a-c). Altogether, these data provide the first evidence that
142 *B. abortus* induces an increase of myeloid cells production in a Omp25/CD150-dependent manner,
143 though not at the expense of lymphoid cells.

144
145 HSCs are known to both self-renew and differentiate in order to replenish the whole hematopoietic
146 system, properties that can be tested by transplantation in an irradiated host [6, 28]. In order to
147 functionally confirm that the increased production of myeloid progenitors and mature cells was
148 initiated by direct stimulation of HSCs by *Brucella*, we co-transplanted *ex vivo* stimulated and
149 unstimulated HSCs in the same recipient. Towards this end we sorted HSCs (KSL, CD48⁻, CD34⁻,
150 CD135⁻) from CD45.1 *CD150*^{-/-} or CD45.1 *wt* mice, stimulated them *ex vivo* with *Brucella* for 30
151 min and treated them with gentamicin to kill extracellular bacteria. We then transplanted the
152 stimulated HSCs together with non-stimulated competitor HSCs (ratio 2:1) into lethally irradiated
153 CD45.2 recipient mice (Fig. 3e). Blood analyses at 4 weeks post-transplantation show that HSCs
154 stimulated with *B. abortus* WT generated more myeloid than lymphoid cells in the peripheral blood,
155 compared to PBS-treated HSCs (Fig. 3f, upper panel and Supplementary Fig.3 for gating strategy).
156 Again, the myeloid commitment bias of hematopoietic stem cells was abolished when HSCs were
157 stimulated *ex vivo* with *B. abortus* $\Delta omp25$ (Fig. 3f, upper panel) or in *CD150*^{-/-} HSCs stimulated
158 with *B. abortus* WT (Fig. 3f, lower panel). Furthermore, the increased myeloid to lymphoid ratio in
159 the blood generated by *B. abortus* WT stimulated HSCs was transient and was not observed at 6-
160 and 8-weeks post-transplantation. This indicates that HSCs re-equilibrate lineage commitment

161 without compromising long-term multi-lineage contribution, as is also observed for direct M-CSF
162 stimulation of HSC [20]. In summary, *in vivo* and *ex vivo* data prove for the first time that HSCs are
163 able to sense directly live bacteria such as *Brucella abortus* via CD150 and transiently increase the
164 production of myeloid cells in response.

165

166 Immune effector cell functions are globally altered in *CD150*^{-/-} mice [29]. We further examined
167 whether, following infection with *Brucella*, the observed lack of HSC myeloid lineage commitment
168 and downstream production of myeloid effectors in *CD150*^{-/-} mice is due to absent CD150-
169 mediated bacterial recognition in HSCs or globally defective innate immune cell effector function.
170 For this, we generated mixed hematopoietic chimera mice by transplanting a 1:1 mix of BM cells
171 from *CD150*^{+/+}; CD45.2 mice and *CD150*^{-/-}; CD45.1 mice into irradiated CD45.2 recipient mice
172 (Fig. 4a). This allowed investigation of both *CD150*^{+/+} HSCs and *CD150*^{-/-} HSCs in the same
173 environment and in the presence of *wt* innate immune cells during infection. At twelve weeks post-
174 transplantation, we infected chimeric mice with *B. abortus*. We then assessed their lineage output in
175 both CD45.2 (*CD150*^{+/+}) and CD45.1 (*CD150*^{-/-}) compartments by analysing the myeloid/lymphoid
176 ratio in mature blood cells and bone marrow progenitors (Fig. 4b-e). At 8 days post-infection with
177 *B. abortus* WT, the blood myeloid/lymphoid ratio was higher in the *wt* compartment compared to
178 the *CD150*^{-/-} compartment (Fig. 4b). The increase of blood myeloid/lymphoid ratio in the *wt*
179 compartment was also abolished upon Ba *Δomp25* infection of chimeric mice (Fig. 4b). In BM
180 progenitor cells, the percentage of GMP (Fig. 4c) and myeloid-biased MPP2-3 cells (Fig. 4d) was
181 also increased in the BM in a *Omp25*/*CD150*-dependent manner. Interestingly, *Omp25*/*CD150*
182 interaction did not perturb the number of lymphoid-biased multipotent progenitors MPP4 (Fig. 4e).
183 These results confirm that myeloid commitment induced by *B. abortus* *Omp25*/*CD150* interaction
184 is intrinsic to HSC.

185 Infection by several pathogens is sometime associated with reduced red blood cell generation
186 leading to a so called acute arrest of hematopoiesis (AAH) [30]. Interestingly, in the *wt* mice
187 infected with *Brucella* the percentage of erythroid progenitors (MEP) in the BM decreased in a

188 Omp25/CD150 dependant manner (Supplementary Fig.4a). To investigate if the reduced level of
189 MEP results in anemia, we infected *wt* and *CD150*^{-/-} mice i.p. with *B. abortus*. At D8 p.i. we
190 measured the hematocrit in the blood of the infected mice (Supplementary Fig.4b). As expected, the
191 hematocrit of infected mice was reduced compared to non-infected mice in an Omp25/CD150-
192 dependent manner (Supplementary Fig.4b).

193 These results indicate that in addition to increased myeloid commitment, reduced production of red
194 cells already at level of progenitors cells is a Omp25/CD150-dependent feature of *Brucella*
195 infection.

196 Notably, anemia associated with a decrease of red blood cells, hematocrit and haemoglobin was
197 detected in 302 human patients (31.8% of men and 25% women) (Supplementary Fig.4c). These
198 clinical data suggest that *Brucella* also alters red cell production in humans as in the mouse model
199 leading to anemia and lack of body oxygenation. This phenomenea is responsible of fatigue,
200 changes in metabolism and sometimes organ damage [31].

201 We also observed a splenomegaly in brucellosis patients, corroborating the results we obtained
202 using the mouse model (Supplementary Fig 3d).

203 In addition, enhanced myeloid commitment has been shown to promote pathogen clearance of *E.*
204 *coli* and *Salmonella* Typhimurium [17]. Nevertheless, for some pathogens, HSPC expansion is
205 detrimental to the host and benefits the pathogen [32]. *CD150*^{-/-} mice are protected from
206 *Trypanosoma cruzi* lethal challenge but are sensitive to *Leishmania major* and to attenuated
207 *Salmonella* Typhimurium [31]. Bacterial load in the spleen of Ba Δ omp25 *wt* infected mice or
208 infected *CD150*^{-/-} mice at 4 weeks post-infection decreased compared to *wt* infected mice (Fig 4g).

209 This suggests that the enhanced transient myeloid commitment induced by Omp25/CD150 benefits
210 the bacterium. Indeed, *Brucella* infects and replicates in myeloid cells [7, 33]. This may be one of
211 the strategies established by *Brucella* to promote chronic infection and help bacterial dissemination.
212 The Omp25/CD150 axis can thus be considered as a new evasion strategy exploited by *B. abortus*
213 to mediate its dissemination. Here, we present the novel finding demonstrating that CD150 is a

214 bacterial sensor for HSC. How chronic activation of HSC by *B. abortus* could affect long-term
215 function of HSC and the role of CD150 in HSC of patients experiencing a microbial challenge
216 would be worth investigating in the future.

217

218 **METHODS**

219 **Ethics**

220 Animal experimentation was conducted in strict compliance with good animal practice as defined
221 by the French Animal Welfare Bodies (Law 87–848 dated 19 October 1987 modified by Decree
222 2001-464 and Decree 2001-131 relative to European Convention, EEC Directive 86/609). INSERM
223 guidelines have been followed regarding animal experimentation (authorization No. 02875 for
224 mouse experimentation). All animal work was approved by the Direction Départementale Des
225 Services Vétérinaires des Bouches du Rhône and the Regional Ethic Committee (authorization
226 number 13.118). Authorisation of *Brucella* experimentation in BSL3 facility was given under the
227 numbers: AMO-076712016-5, AMO-076712016-6 and AMO-076712016-7. All efforts were made
228 to minimize suffering during animal handling and experimentation.

229 The study in humans was approved by the Ethics Committee of the Medical Faculty in Skopje,
230 Republic of North Macedonia (No 03-7670/2).

231 Human study:

232 The values of red blood cells, hematocrit and haemoglobin were retrospectively analyzed in 302
233 patients with human brucellosis before therapy was initiated. The patients were managed at the
234 University clinic of infectious diseases and febrile conditions in Skopje from 2007 to 2018. Males
235 were 217 and females 85 of them with a median age of 39 (range 3-79) years. The diagnosis of
236 brucellosis was based on clinical findings compatible with brucellosis (arthralgia, fever, sweating,
237 malaise, hepatomegaly, splenomegaly, signs of focal disease), confirmed by a qualitative positive
238 Rose Bengal test and a Brucellacapt assay of $>1/320$. Hemoglobin thresholds used to define anemia
239 were according to World Health Organization [World Health Organization (2008)]. Worldwide

240 prevalence of anaemia 1993–2005 (PDF). Geneva: World Health Organization. ISBN 978-92-4-
241 159665-7. Archived (PDF) from the original on 12 March 2009. Retrieved 2009-03-25].

242

243

244

245 **Mice**

246 6-10 week-old female C57BL/6J mice from Charles River, *CD150*^{-/-} mice (kindly provided by
247 Yusuke Yanagi) [29] or Pu.1^{+GFP} mice [21, 22], both on a C57BL/6J background, were used.
248 Animals were housed in cages with water and food *ad libitum* in the CIPHE animal house facility,
249 Marseille. Two weeks before the start of experiments, mice were transferred to the BSL3, CIPHE,
250 Marseille, and kept under strict biosafety containment conditions all along infection with live
251 bacteria.

252

253 **Bacterial strains**

254 *Brucella abortus* 2308 (Ba WT), *Brucella abortus* Δ omp25 (kanR) (Ba Δ omp25), or *Brucella*
255 *abortus* Δ omp25c:pOmp25 (kanR, AmpR) (Ba Δ omp25c) were used for infection. Ba Δ omp25 was
256 a gift from Pr. Ignacio Moriyón, University of Navarra.

257 ***Brucella* infection**

258 Mice were inoculated intraperitoneally with 1×10^6 CFU in 100 μ l of PBS for each *Brucella* strain.
259 Strains were grown in Tryptic Soy Agar (Sigma Aldrich) for 5 days, then overnight at 37°C for 16 h
260 under shaking in Tryptic Soy Broth (Sigma Aldrich) with kanamycin for Ba Δ omp25 until the OD
261 (OD at 600nm) reached 1.8 and with 25 μ g/mL for the Ba Δ omp25 strain or kanamycin and
262 ampicillin 50 μ g/mL for the Ba Δ omp25pBBR4omp25 strain. All *Brucella* were kept, grown and
263 used under strict biosafety containment conditions all along experiments in the BSL3 facility,
264 Marseille. For Colony Forming Units (CFU) enumeration at different time points post-infection,
265 spleen and bone marrow were collected [7]. Femur and tibia were flushed with 500 μ l of ice-cold

266 PBS to isolate BM cells. BM cell suspension was then plated in TSA plates. Spleens were collected
267 and splenocytes were isolated by mechanical disruption.
268 Organs were harvested at 2, 8 or 30 days post-infection, weighted and then dissociated into sterile
269 endotoxin free PBS. Serial dilutions in sterile 1xPBS were used to count CFU. Serial dilutions were
270 plated in triplicates onto TSB agar to enumerate CFU after 3 days at 37°C.

271

272

273 **Transplantation assay**

274 All donor cells were from *CD150^{+/+}* and *CD150^{-/-}* CD45.1 mice and transplanted into lethally
275 irradiated (5,9 Gy) CD45.2 recipient mice. For competitive assays, mice were transplanted with
276 equal numbers of 1×10^6 total BM cells or 1×10^6 lineage negative cells. For infected HSC
277 transplantation, 1000 Sorted HSC (KSL, CD48⁻, CD135⁻, CD34⁻) were infected with Ba *WT* or Ba
278 *Δomp25* at a MOI of 30:1. Bacteria were centrifuged onto cells at 400 g for 10 min at 15°C and then
279 incubated for 45 min at 37°C under 5% CO₂. Cells were washed twice with medium and then
280 incubated for 1 h in medium containing 100 μg/ml gentamicin (Sigma Aldrich) to kill extracellular
281 bacteria. Cells were then washed 3 times with PBS. Infected cells were mixed in a ratio (2:1) with
282 non-infected HSC before transplantation. Haematopoietic reconstitution and lineage determination
283 were monitored at 4 weeks, 6 weeks and 8 weeks post-transplantation in the peripheral blood. At 8
284 weeks post-transplantation mice were sacrificed and tibia and femurs were harvested. BM cells were
285 flushed from femur and tibia and resuspended in FACS media (PBS, 2%FCS, 5mm EDTA) for
286 Flow Cytometry analyses.

287

288 **Flow Cytometry**

289 For FACS sorting and analysis we used a FACSAriaIII or a LSR-X20 (BD) and the FlowJo
290 software v10 (Treestar). For HSC and progenitor analysis, total BM cells were depleted of mature
291 cells using a direct lineage depletion kit (Miltenyi Biotec) and stained with antibodies anti-CD34-
292 APC or anti-BV421 (BD Bioscience, cloneRAM34), anti-CD135-PE-CF594 or anti-PE (BD

293 Bioscience, clone A2F10.1), anti-CD150-PE-Cy7 or anti-BV711 (BioLegend, clone TC15-
294 12F12.2), anti-CD117-BV605 (BioLegend, clone 2B8), anti-Sca-1-PrpcCy5.5 or anti-PE
295 (ThermoFischer Scientist, clone D7), anti-CD48-BV510 or anti-PE-Cy7 (BD Bioscience, clone
296 HM48-1), anti-CD16/32-PE or anti-APC-Cy7 (BD Bioscience, clone 2.4G2). When needed, anti-
297 CD45.1-APC or anti-BV421 (BD Bioscience, clone A20) and anti-CD45.2-FITC or anti-PrpcCy5.5
298 (BD Bioscience, clone 104) were added. LIVE/DEAD (UV Fixable Blue Dead Cell Stain,
299 ThermoFischer) was used as viability marker.

300 Blood cells were stained with anti-CD11b FITC (eBioscience, clone M1/70), anti-CD19-PE-Cy7
301 (BioLegend, clone 6D5), anti-CD45.2-PrpcCy5.5 (BD Bioscience, clone 104), anti-CD45.1-BV421
302 (BD Bioscience, clone A20), anti-CD3e-APC (BD Bioscience, clone 145-2C11) and anti-Ly6G-PE
303 (BD Bioscience, clone 1A8). Red blood cells were lysed using BD FACS lysing solution (BD) for
304 10 min then fixed for 20 min with Antigen Fix, prior to acquisition.

305

306 **Haematopoietic Stem Cells *ex vivo* challenge with *Brucella abortus* membrane extracts**

307 All cultures were performed at 37°C under 5% CO₂. Sorted HSC from wt or *CD150*^{-/-} mice were
308 cultured in StemSpan SFEMII (Stem Cells) complemented with 50 ng/μL TPO (Peprotech) and 20
309 ng/μL SCF (Peprotech). Cells were stimulated with *Brucella* membrane extracts from Ba WT or
310 with Ba *Δomp25* (10 μg/ml). *Brucella* membrane extracts were a gift from Pr. I. Moriyon,
311 University of Navarra.

312 Sorted HSC were also cultured with blocking CD150 peptide (FCKQLKLYEQVSPPE, Auspep,
313 100 μg/ml) or control peptide (DLSKGSYPDHLEDGY, Auspep, 100 μg/ml) (Thermo Scientific).

314

315 **Statistics**

316 Results were evaluated by GraphPad Prism v8 software (GraphPad Software, San Diego, CA, USA)
317 using. Statistical tests used are indicated in the figure legends. The value of *P < 0.05 was
318 determined as significant.

319

320 **DATA AVAIBILITY**

321 No datasets were generated during the current study.

322

323 REFERENCES

- 324 1. Nebe, C.T., et al., *Detection of Chlamydophila pneumoniae in the bone marrow of two*
325 *patients with unexplained chronic anaemia*. European journal of haematology, 2005.
326 **74**(1): p. 77-83.
- 327 2. Eldin, C., et al., *18F-FDG PET/CT as a central tool in the shift from chronic Q fever to*
328 *Coxiella burnetii persistent focalized infection: A consecutive case series*. Medicine, 2016.
329 **95**(34).
- 330 3. Allen, M.B., et al., *First reported case of Ehrlichia ewingii involving human bone marrow*.
331 J Clin Microbiol, 2014. **52**(11): p. 4102-4.
- 332 4. Hardy, J., P. Chu, and C.H. Contag, *Foci of Listeria monocytogenes persist in the bone*
333 *marrow*. Dis Model Mech, 2009. **2**(1-2): p. 39-46.
- 334 5. Reece, S.T., et al., *Mycobacterium tuberculosis-Infected Hematopoietic Stem and*
335 *Progenitor Cells Unable to Express Inducible Nitric Oxide Synthase Propagate*
336 *Tuberculosis in Mice*. J Infect Dis, 2018. **217**(10): p. 1667-1671.
- 337 6. Weissman, I.L., *Clonal origins of the hematopoietic system: the single most elegant*
338 *experiment*. The Journal of Immunology, 2014. **192**(11): p. 4943-4944.
- 339 7. Gutierrez-Jimenez, C., et al., *Persistence of Brucella abortus in the Bone Marrow of*
340 *Infected Mice*. J Immunol Res, 2018. **2018**: p. 5370414.
- 341 8. Franco, M.P., et al., *Human brucellosis*. The Lancet Infectious Diseases, 2007. **7**(12): p.
342 775-786.
- 343 9. Boettcher, S., et al., *Endothelial cells translate pathogen signals into G-CSF-driven*
344 *emergency granulopoiesis*. Blood, 2014. **124**(9): p. 1393-403.
- 345 10. Boettcher, S. and M.G. Manz, *Regulation of Inflammation- and Infection-Driven*
346 *Hematopoiesis*. Trends Immunol, 2017. **38**(5): p. 345-357.
- 347 11. Kiel, M.J., et al., *SLAM family receptors distinguish hematopoietic stem and progenitor*
348 *cells and reveal endothelial niches for stem cells*. Cell, 2005. **121**(7): p. 1109-21.
- 349 12. Berger, S.B., et al., *SLAM is a microbial sensor that regulates bacterial phagosome*
350 *functions in macrophages*. Nat Immunol, 2010. **11**(10): p. 920-7.
- 351 13. Degos, C., et al., *Omp25 - dependent engagement of SLAMF1 by Brucella abortus in*
352 *dendritic cells limits acute inflammation and favours bacterial persistence in vivo*.
353 Cellular Microbiology, 2020.
- 354 14. Takizawa, H., et al., *Pathogen-Induced TLR4-TRIF Innate Immune Signaling in*
355 *Hematopoietic Stem Cells Promotes Proliferation but Reduces Competitive Fitness*. Cell
356 Stem Cell, 2017. **21**(2): p. 225-240 e5.
- 357 15. Mitroulis, I., et al., *Modulation of Myelopoiesis Progenitors Is an Integral Component of*
358 *Trained Immunity*. Cell, 2018. **172**(1-2): p. 147-161 e12.

- 359 16. Kobayashi, H., et al., *Bacterial c-di-GMP affects hematopoietic stem/progenitors and*
360 *their niches through STING*. Cell Rep, 2015. **11**(1): p. 71-84.
- 361 17. Takizawa, H., S. Boettcher, and M.G. Manz, *Demand-adapted regulation of early*
362 *hematopoiesis in infection and inflammation*. Blood, 2012. **119**(13): p. 2991-3002.
- 363 18. Pronk, C.J., et al., *Tumor necrosis factor restricts hematopoietic stem cell activity in mice:*
364 *involvement of two distinct receptors*. Journal of Experimental Medicine, 2011. **208**(8):
365 p. 1563-1570.
- 366 19. Pietras, E.M., *Inflammation: a key regulator of hematopoietic stem cell fate in health and*
367 *disease*. Blood, 2017. **130**(15): p. 1693-1698.
- 368 20. Mossadegh-Keller, N., et al., *M-CSF instructs myeloid lineage fate in single*
369 *haematopoietic stem cells*. Nature, 2013. **497**(7448): p. 239-43.
- 370 21. Back, J., et al., *PU. 1 determines the self-renewal capacity of erythroid progenitor cells*.
371 Blood, 2004. **103**(10): p. 3615-3623.
- 372 22. Bryder, D., D.J. Rossi, and I.L. Weissman, *Hematopoietic stem cells: the paradigmatic*
373 *tissue-specific stem cell*. The American journal of pathology, 2006. **169**(2): p. 338-346.
- 374 23. Kobayashi, H., et al., *Bacterial c-di-GMP affects hematopoietic stem/progenitors and*
375 *their niches through STING*. Cell reports, 2015. **11**(1): p. 71-84.
- 376 24. Burberry, A., et al., *Infection mobilizes hematopoietic stem cells through cooperative*
377 *NOD-like receptor and Toll-like receptor signaling*. Cell Host Microbe, 2014. **15**(6): p.
378 779-91.
- 379 25. Kiel, M.J., et al., *SLAM Family Receptors Distinguish Hematopoietic Stem and Progenitor*
380 *Cells and Reveal Endothelial Niches for Stem Cells*. Cell, 2005. **121**(7): p. 1109-1121.
- 381 26. Boigegrain, R.A., et al., *Release of periplasmic proteins of Brucella suis upon acidic shock*
382 *involves the outer membrane protein Omp25*. Infect Immun, 2004. **72**(10): p. 5693-703.
- 383 27. Essers, M.A., et al., *IFNalpha activates dormant haematopoietic stem cells in vivo*. Nature,
384 2009. **458**(7240): p. 904-8.
- 385 28. Till, J.E. and E.A. McCulloch, *A direct measurement of the radiation sensitivity of normal*
386 *mouse bone marrow cells*. Radiation research, 1961. **14**(2): p. 213-222.
- 387 29. Davidson, D., et al., *Genetic evidence linking SAP, the X-linked lymphoproliferative gene*
388 *product, to Src-related kinase FynT in T(H)2 cytokine regulation*. Immunity, 2004.
389 **21**(5): p. 707-17.
- 390 30. Bi, L., et al., *Acute arrest of hematopoiesis induced by infection with Staphylococcus*
391 *epidermidis following total knee arthroplasty: A case report and literature review*. Exp
392 Ther Med, 2016. **11**(3): p. 957-960.
- 393 31. Silverberg, D.S., et al., *The pathological consequences of anaemia*. Clin Lab Haematol,
394 2001. **23**(1): p. 1-6.
- 395 32. Abidin, B.M., et al., *Infection-adapted emergency hematopoiesis promotes visceral*
396 *leishmaniasis*. PLoS Pathog, 2017. **13**(8): p. e1006422.

397 33. Salcedo, S.P., et al., *BtpB, a novel Brucella TIR-containing effector protein with immune*
398 *modulatory functions*. *Frontiers in Cellular and Infection Microbiology*, 2013. **3**.

399

400 **ACKNOWLEDGEMENTS**

401 We thank all the staff of the CIML and CIPHE mouse houses, Atika Zouine, Marc Barad, and
402 Sylvain Bigot of the CIML flow cytometry facility, Dr. Hervé Luche, Pierre Grenot of the CIPHE
403 flow cytometry facility, Claude Napez and Philippe Hoest of the CIPHE BSL-3 facility. We
404 acknowledge Pr. Ignacio Moriyon (University of Pamplona, France) for generous gift of
405 mutant *Brucella* strains and Dr. Yusuke Yanagi and Dr. Masato Kubo for providing us with
406 *CD150^{-/-} CD45.1* mice. We thank Dr. Taymour Hamoudi from University of California San
407 Francisco for critical reading of the manuscript and Dr. Sylvie Memet and Dr. Guillaume
408 Hoeffel for discussions about this work.

409 This study was supported by institutional grants from the Institut National de la Santé et de la
410 Recherche Médicale, Centre National de la Recherche Scientifique, and Aix-Marseille
411 University to CIML and grants to JPG from Fondation pour la Recherche médicale (FRM grant
412 number [DQ20170336745](#)), the Agence Nationale de Recherche/Investissements d’Avenir–
413 Labex INFORM (ANR-11-LABX-0054) and Agence Nationale de Recherche/Investissements
414 d’Avenir–A*MIDEX (ANR-11-IDEX-0001-02), to SS from ITMO Cancer Aviesan (Alliance
415 Nationale pour les Sciences de la Vie et de la Santé, National Alliance for Life Science and
416 Health) within the framework of the Cancer Plan (ISC19032ASA) and to M.H. Sieweke from
417 the Agence Nationale pour la Recherche (ANR-17-CE15-0007-01 and ANR-18-CE12-0019-03),
418 Fondation ARC pour la Recherche sur le Cancer (PGA1 RF20170205515), an INSERM–
419 Helmholtz cooperation and the European Research Council (ERC) under the European Union’s
420 Horizon 2020 research and innovation program (grant agreement number 695093 MacAge).
421 LH received a fellowship from Investissements d’Avenir–Labex INFORM, BDL received a
422 fellowship from the Fondation ARC. M.H. Sieweke was supported as a Berlin Institute of

423 Health Einstein visiting fellow at MDC and is an Alexander von Humboldt Professor at TU
424 Dresden.

425

426 **AUTHORS CONTRIBUTION**

427 J.P.G, M.S, S.S conceived and J.P.G, S.S supervised the study. J.P.G , M.S, S.S, B.D.L, L.H, V.A
428 design the experiments. L.H, G.G. and V.A performed all BSL-3 experiments and B.D.L and G.D
429 performed experiments not requiring a BSL-3 facility. M.B was responsible of human studies.
430 J.P.G, M.S, S.S, B.D.L, L.H, V.A interpreted the data. J.P.G , M.S, S.S, B.D.L, L.H, V.A wrote the
431 manuscript

432

433 **DECLARATION OF INTERESTS**

434 The authors declare no competing interests.

435

436 FIGURES LEGENDS

437 **Figure 1: *Brucella abortus* persists in the BM and affects HSPC homeostasis.**

438 a) Experimental scheme: Mice were intraperitoneally inoculated with 1×10^6 CFU of wild-type *B.*
439 *abortus*. BM cells were isolated from femur and tibia of the infected mice, resuspended in PBS and
440 transplanted into previously lethally irradiated mice. 8 weeks after transplantation CFU per gram of
441 organ were enumerated from spleens and bone marrow (BM). b) Enumeration of CFUs per gram of
442 spleen and BM at 8 weeks post transplantation (n=7). c-d) C57BL/6J wild-type (*wt*) mice were
443 intraperitoneally inoculated with 1×10^6 CFU of wild-type *B. abortus*. Two, eight and thirty days
444 later, FACS analyses were performed for BM cells. Representative FACS profiles (d) and frequency
445 of LSK ($\text{lin}^-, \text{Sca}^+, \text{cKit}^+$) (from left to right, n=30 ; 15 ; 21), LSK CD48⁺ ($\text{lin}^-, \text{Sca}^+, \text{cKit}^+ \text{CD48}^+$)
446 (from left to right, n=28 ; 14 ; 17), LSK CD48⁻ ($\text{lin}^-, \text{Sca}^+, \text{cKit}^+ \text{CD48}^-$) (from left to right, n=30 ; 17
447 ; 20), LSK CD48⁻ CD34⁺ ($\text{lin}^-, \text{Sca}^+, \text{cKit}^+ \text{CD48}^-, \text{CD34}^+, \text{CD135}^-$) (from left to right, n=24 ; 14 ;
448 19), HSCST ($\text{lin}^-, \text{Sca}^+, \text{cKit}^+ \text{CD48}^-, \text{CD135}^- \text{CD34}^-, \text{CD150}^-$) (from left to right, n=25 ; 17 ; 16),
449 HSC^{LT} ($\text{lin}^-, \text{Sca}^+, \text{cKit}^+ \text{CD48}^-, \text{CD135}^- \text{CD34}^-, \text{CD150}^+$) (from left to right, n=22 ; 17 ; 22) in
450 lineage negative fraction of BM (c) for PBS treated (Mock ○) and infected mice (■). Data were
451 obtained from distinct samples and from
452 5 independent experiments, each with at least n=3 animals per condition, are shown and mean
453 \pm SEM is represented by horizontal bar. Significant differences from mock are shown. *** $P <$
454 0.001, ** $P <$ 0.01, * $P <$ 0.05. Absence of P value or ns, non-significant. Since data followed
455 normal distribution, P-Value were generated using Brown-Forsyth followed by ANOVA Welch test.

456

457 **Figure 2: *Brucella* induces PU.1 upregulation in a Omp25/CD150 dependent manner**

458 a) Experimental scheme $Pu.1^{+/GFP}$ and $CD150^{-/-} Pu.1^{+/GFP}$ mice were intraperitoneally injected with
459 PBSx1 (Mock, ○) or inoculated with 1×10^6 CFU of wild-type *B. abortus* (Ba WT, ■), Ba Δomp25
460 (■). Two days after, the percentage of GFP expression in HSCs ($\text{lin}^-, \text{Sca}^+, \text{cKit}^+ \text{CD48}^-, \text{CD135}^-$
461 CD34^-) was assessed by Flow Cytometry. b) GFP expression in BM HSCs ($\text{lin}^-, \text{Sca}^+, \text{cKit}^+ \text{CD48}^-$,
462 $\text{CD135}^- \text{CD34}^-$) assessed by Flow Cytometry at D2 p.i.. Data (b) were obtained from distinct
463 samples (from left to right, n=5 ; 10 ; 5 ; 5 ; 6) from 3 independent experiments. Mean \pm SD is
464 represented by horizontal bar. Significant differences from mock are shown. *** $P <$ 0.001, ** $P <$
465 0.01, * $P <$ 0.05. Absence of P value or ns, non-significant. Since data did not follow normal
466 distribution, P-Value were generated using Kruskal-Wallis followed by Dunn's test. c) Experimental
467 scheme: HSC ($\text{lin}^-, \text{Sca}^+, \text{cKit}^+ \text{CD48}^-, \text{CD135}^- \text{CD34}^-$) from $Pu.1^{+/GFP}$ or $CD150^{-/-} Pu.1^{+/GFP}$ mice
468 were sorted, then stimulated *ex vivo* with PBSx1 or *B. abortus* WT OMVs, *B. abortus* Δomp25
469 OMVs. After 16h, the level of GFP in cells was assessed by Flow Cytometry. d) Fold change ratio

470 of GFP expression in HSC 16 hours after *ex vivo* stimulation with *B. abortus* WT OMVs (■), *B.*
471 *abortus* $\Delta omp25$ OMVs (■) compared to mock (Mock, ○) assessed by Flow Cytometry (from left
472 to right, n=6 ; 6 ; 6 ; 5 ; 5). e) Percentage of GFP⁺ HSC assessed by Flow Cytometry 0h (Mock, ○,
473 n=4) or 16h after *ex vivo* stimulation with *B. abortus* WT (■, n=4), *B. abortus* WT OMVs and the
474 control peptide (100µg/ml) (■, n=2) and blocking peptide of CD150 (100µg/ml) (■, n=2). Data (e,
475 f) were
476 obtained from HSC of a pool of 3-4 mice, the pool of cells have been divided by the number of
477 tested conditions. Each dot is a replicative experiment. Mean \pm SD is represented by horizontal
478 bar. Significant differences from mock are shown. ** P< 0.01, * P< 0.05. P-Value were
479 generated using Mann Whitney test.

480

481 **Figure 3: *B. abortus* induces HSC differentiation towards myeloid lineage.**

482 **a-d)** C57BL/6J wild-type (*wt*) and *CD150*^{-/-} mice were intraperitoneally inoculated with 1×10^6 *B.*
483 *abortus* CFUs. Eight days later, FACS analyses were performed for BM cells. Frequency of (a)
484 MPP2-3 (lin⁻, Sca⁺, cKit⁺ CD48⁺, CD135⁻) (from left to right : n=22 ; 19 ; 14 ; 6 ; 11; 9 ; 8), (b)
485 MPP4 (lin⁻, Sca⁺, cKit⁺ CD48⁺, CD135⁺) (from left to right : n=22 ; 21 ; 12 ; 4 ; 9 ; 9 ; 9), (c) GMP
486 (lin⁻, Sca⁻, cKit⁺ CD34⁺, CD16/32⁺) (from left to right : n=16 ; 18 ; 13 ; 4 ; 8 ; 9 ; 9), in Lin⁻ BM cells
487 is shown for (Mock, ○) or inoculated with 1×10^6 CFU of wild-type *B. abortus* (Ba WT, ■), *B.*
488 *abortus* $\Delta omp25$ (Ba $\Delta omp25$ ■) or *B. abortus* $\Delta omp25$ complemented with p:Omp25 (Ba
489 $\Delta omp25c$ □) mutants (the latter only for *wt* mice). d) Eight days post-infection, myeloid cells
490 (CD45⁺, CD11b⁺) to lymphoid cells (CD3e⁺CD19⁺) ratio in blood is shown for (Mock, ○, n=11) or
491 inoculated with 1×10^6 CFU of *wild-type B. abortus* (Ba WT, ■, n=9), *B. abortus* $\Delta omp25$ (Ba
492 $\Delta omp25$ ■). e) Experimental scheme: HSC from *wt* CD45.1 and *CD150*^{-/-} CD45.1 mice were
493 sorted and then incubated *ex vivo* with *B. abortus* WT and *B. abortus* $\Delta omp25$ for 30 minutes. After
494 30 minutes, cells were washed and treated for 1 hour with gentamycin to kill extra-cellular bacteria.
495 HSC were then transplanted into lethally irradiated *wt* CD45.2 recipients. FACS analyses of blood
496 samples were performed at 4, 6 and 8 weeks post-transplantation. f) myeloid cells (CD45⁺,
497 CD11b⁺) to lymphoid cells (CD3e⁺CD19⁺) ratio in CD45.1⁺ blood cells is shown for hematopoietic
498 cells provided by CD45.1⁺ *wt* mice (upper panel) or *CD150*^{-/-} mice, (lower panel) , non-infected
499 (Mock, ○) or infected with 1×10^6 CFU of wild-type *B. abortus* (Ba WT, ■), *B. abortus* $\Delta omp25$
500 (Ba $\Delta omp25$ ■) as described in e (from left to right, for WT n=12 ; 13 ; 10 ; 10 ; 9 ; 9 ; 12 ; 8 ; 8 and
501 for *CD150*^{-/-} n= 9 ; 4 ; 14 ;
502 8 ; 11 ; 7). Data were obtained from distinct samples from 4 independent experiments (a-d) or
503 from repetitive sampling from 2 (e-f) independent experiments. Mean \pm SEM is represented by
504 horizontal bar. Significant differences from mock are shown. *** P< 0.001, ** P< 0.01, * P<

505 0.05. Absence of P value or ns, non-significant. Since data did not follow normal distribution,
506 P-Value were generated using Kruskal-Wallis followed by Dunn's test.

507

508 **Figure 4: HSC myeloid bias induced by *Brucella* Omp25/CD150 interaction is hematopoietic**
509 **cell autonomous.**

510 **a)** Experimental scheme: BM cells from *CD150*^{-/-} CD45.1 mice and *wt* CD45.2 mice were isolated
511 from tibia and femur of mice and transplanted into lethally irradiated recipient mice. Twelve weeks
512 after transplantation mice were intraperitoneally injected with PBSx1 (Mock, ○) or inoculated with
513 1x10⁶ CFU of wild-type *B. abortus* (Ba WT), *B. abortus* Δ omp25 (Ba Δ omp25). Blood and BM
514 were analysed 8 days after. **b)** Myeloid (CD45⁺, CD11b⁺ cells) to lymphoid (CD3e⁺ and CD19⁺
515 cells) in the blood (from left to right, n=8 ; 8 ; 8 ; 8 ; 7 ; 7); frequency of **c)** GMP (from left to right,
516 n=6 ; 6 ; 7 ; 7 ; 9 ; 9), **d)** MPP2-3 (from left to right, n=6 ; 6 ; 6 ; 6 ; 9 ; 9) and **e)** MPP4 (from left to
517 right, n=6 ; 6 ; 8 ; 8 ; 9 ; 9) in BM Lin⁻ cells of *wt* (circle) and *CD150*^{-/-} (square) compartment is
518 shown for chimeric mice intraperitoneal injected with PBS (Mock, non-filled symbols) or
519 inoculated with 1x10⁶ CFU of wild-type *B. abortus* (symbol filled in black) *B. abortus* Δ omp25
520 (symbol filled in grey) as described in a. **e-f)** CFU count per gram of organ at Day 30 post infection
521 of WT and *CD150*^{-/-} mice for (e) BM (from left to right n=18 ; 9 ; 8 ; 12 ; 6 ; 6) and (f) spleen
522 (from left to right n= 14 ; 18 ; 7 ; 7 ; 8 ; 6) infected with *B. abortus* WT (Ba WT ■), *B. abortus*
523 Δ omp25 (Ba Δ omp25 ■) or *B. abortus* Δ omp25 complemented with p:Omp25 (Ba Δ omp25c □).
524 Mean \pm SEM is represented by horizontal bar. Significant differences from mock are shown. *** P<
525 0.001, ** P< 0.01, * P< 0.05. Absence of P value or ns, non-significant. Since data did not follow
526 normal distribution, P-Value were generated using Kruskal-Wallis followed by Dunn's test.

527

528 **Supplementary 1: *Brucella* infection does not affect the number of lineage negative**
529 **progenitors and BM cells**

530 **a-b)** *wt* and *CD150*^{-/-} mice were intraperitoneally injected with PBS or inoculated with 1x10⁶ CFU
531 of *B. abortus*. Eight days later, BM cells were isolated, cells were counted (**a**) and then depleted for
532 mature hematopoietic cells as shown in Methods. Lin⁻ cells (**b**) were also counted for (Mock, ○) or
533 infected *B. abortus* (Ba WT, ■), *B. abortus* Δ omp25 (Ba Δ omp25 ■) or *B. abortus* Δ omp25
534 complemented with p:Omp25 (Ba Δ omp25c □) mutants (the latter only for *wt* mice). From left to
535 right, for BM, n=11 ; 14 ; 8 ; 5 ; 9 ; 11 ; 9 and for Lin⁻ BM, n=18 ; 16 ; 8 ; 6 ; 6 ; 7 ; 9. Data
536 obtained from distinct samples from 5 independent experiments.

537 Mean \pm SEM is represented by horizontal bar. Significant differences from mock are shown. ***
538 P<0.001, ** P< 0.01, * P< 0.05. Absence of P value or ns, non-significant. Since data did not follow
539 normal distribution, P-Value were generated using Kruskal-Wallis followed by Dunn's test. c)

540 Complete FACS gating for analysis of HSC and progenitors from lineage negative fraction of BM.
541 First, cells are gated based on SSC/ FSC and then single cells were selected. Viable cells were gated
542 using UV Fixable Blue Dead stain. Described population are : LSK (lin^- , Sca^+ , $cKit^+$), HSCLT (lin^-
543 , Sca^+ , $cKit^+$ $CD48^-$, $CD135^-$ $CD34^-$, $CD150^+$), MPP2-3 (lin^- , Sca^+ , $cKit^+$ $CD48^+$, $CD135^-$), MPP4 (lin^-
544 , Sca^+ , $cKit^+$ $CD48^+$, $CD135^+$), GMP (lin^- , Sca^- , $cKit^+$, $CD34^+$, $CD16/32^+$) and MEP (lin^- , Sca^- , $cKit^+$,
545 $CD34^-$, $CD16/32^-$).

546

547 **Supplementary 2: Infection burden in *Pu.1*^{+GFP} mice**

548 **a-b)** CFU count per gram of organ at Day 2 post infection as described in Fig 2.a. for **(a)** spleen
549 (from left to right n=10 ; 6 ; 6 ; 8) and **(b)** BM (from left to right n=7 ; 6 ; 7 ; 7) of PBS injected
550 (Mock, ○) or infected with *B. abortus* WT (Ba WT, ■), *B. abortus* $\Delta omp25$ (Ba $\Delta omp25$ ■)
551 *Pu.1*^{+GFP} and *CD150*^{-/-} *Pu.1*^{+GFP} mice. Data obtained from distinct samples from 3 independent
552 experiments. Mean \pm SEM is represented by horizontal bar. Significant differences from mock are
553 shown. *** P< 0.001, ** P< 0.01, * P< 0.05. Absence of P value or ns, non-significant. Since data
554 did not follow normal distribution, P-Value were generated using Kruskal-Wallis followed by
555 Dunn's test.

556

557 **Supplementary 3: FACS gating for blood analysis from chimeric mice**

558 Complete FACS gating for blood lineage output from chimeric mice. First, cells are gated based on
559 SSC/ FSC and then single cells were selected. *CD150*^{-/-} and WT cells were separated by gating on
560 respectively CD45.1 and CD45.2 positive cells. In each, lymphoid cells were isolated by gating on
561 CD11b negative cells and then, B cells are CD19 positive cells and T cells are CD3e positive cells.
562 In Cd11b positive cells, granulocytes and monocytes are distinguished by gating onto respectively
563 LY6G positive and negative cells.

564

565 **Supplementary 4: Brucellosis induces anemia.**

566 **a-b)** *wt* *CD45.1* and *CD150*^{-/-} *CD45.1* mice were intraperitoneally inoculated with 1×10^6 CFU of *B.*
567 *abortus*. BM cells were isolated from femur and tibia of the infected mice. a) Frequency of **MEP**
568 (lin^- , Sca^- , $cKit^+$ $CD34^-$ $CD16/32^-$), in Lin^- BM cells is shown for (Mock, ○) or inoculated with
569 1×10^6 CFU of wild-type *B. abortus* (Ba WT, ■), *B. abortus* $\Delta omp25$ (Ba $\Delta omp25$ ■) or *B. abortus*
570 $\Delta omp25$ complemented with p:Omp25 (Ba $\Delta omp25c$ □) mutants (the latter only for wt mice) (from
571 left to right : n=16 ; 16 ; 8 ; 8 ; 8 ; 7 ; 9). **b)** At eight days post-infection, the percentage of
572 haematocrit measured in blood is shown for (Mock, ○) or inoculated with 1×10^6 CFU of *wild-type*
573 *B. abortus* (Ba WT, ■), *B. abortus* $\Delta omp25$ (Ba $\Delta omp25$ ■) (from left to right, n= 7 ; 7 ; 6 ; 5 ; 8 ;
574 8). **c)** Percentage of brucellosis patients that present anemia before antibiotic treatment. Men upper

575 panel and women lower panel. Anemia was characterized by a decrease of hematocrit, hemoglobin
576 and erythrocytes (hematocrit <40% for men and <35% for women; hemoglobin <14g/dL for men
577 and <12 g/dL for women, erythrocyte count <4 million for men and <3.8 million/mm³ for women).
578 Data were obtained from distinct samples from 3 independent experiments (a-b), each with at least
579 n=4 animals per condition, are shown and mean ± SEM is represented by horizontal bar. Significant
580 differences from mock are shown. *** P< 0.001, ** P< 0.01, * P< 0.05. Absence of P value or ns,
581 non-significant. Since data did not follow normal distribution, P-Value were generated using
582 Kruskal-Wallis followed by Dunn's test.

Fig.1

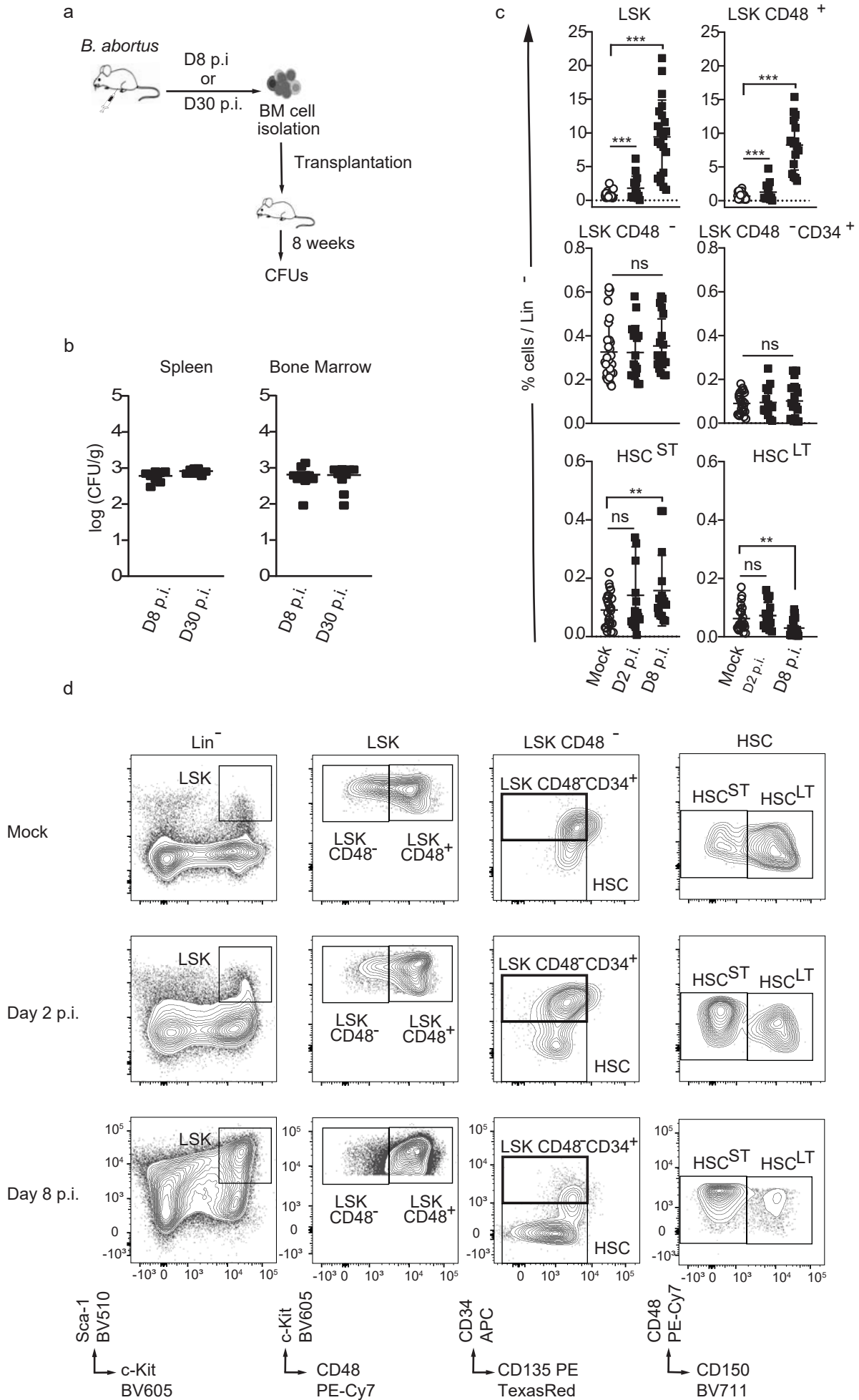
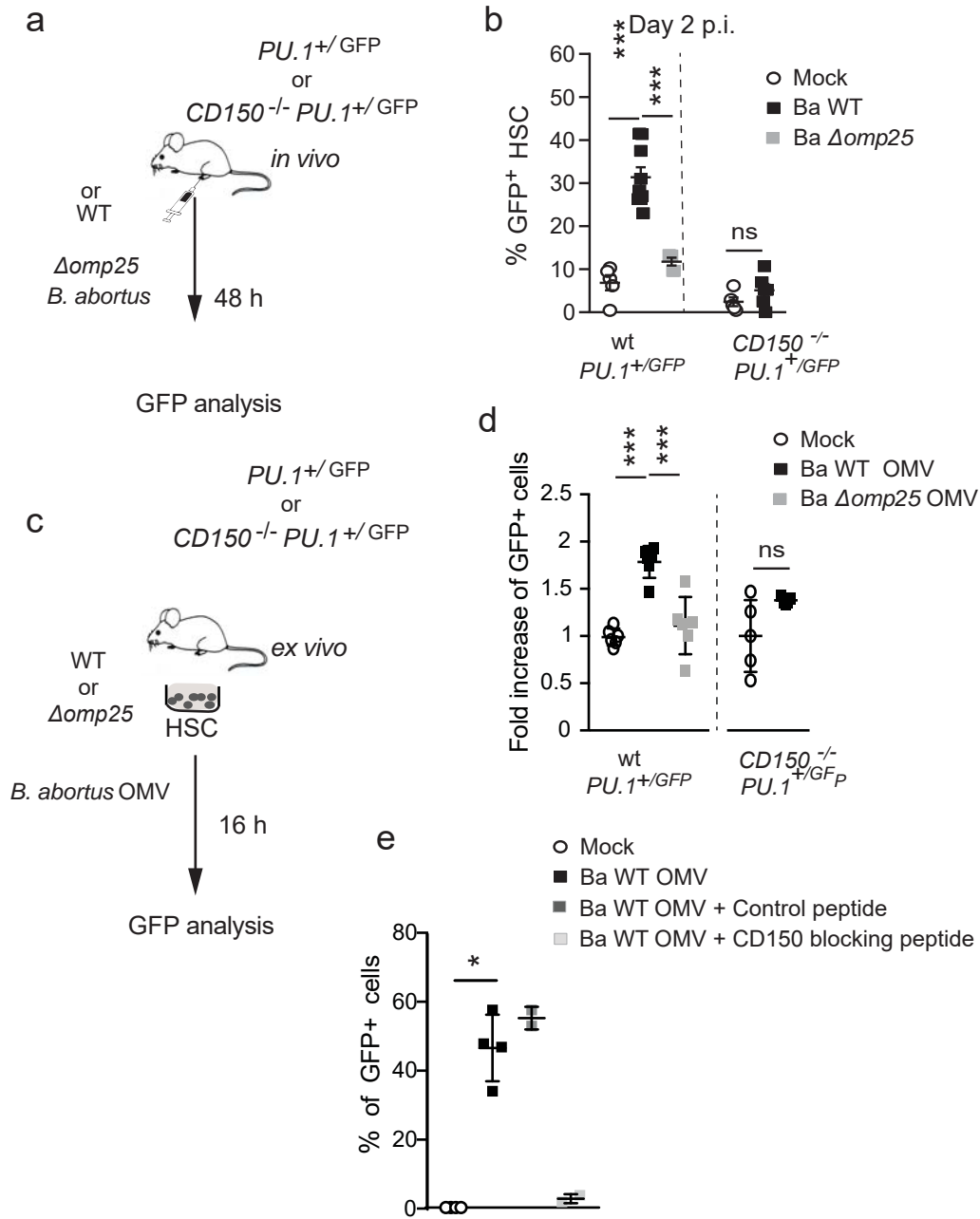


Fig.2



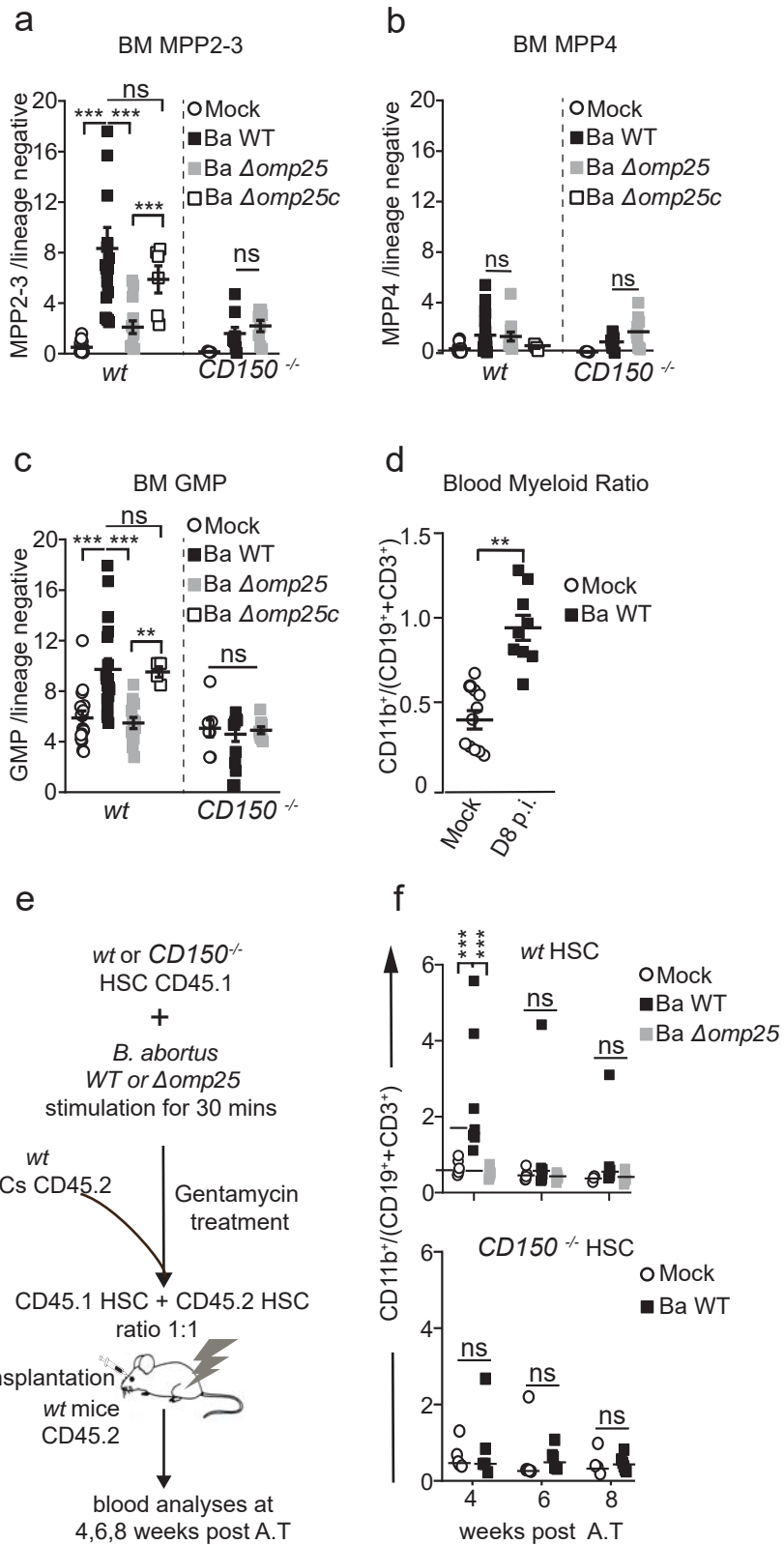
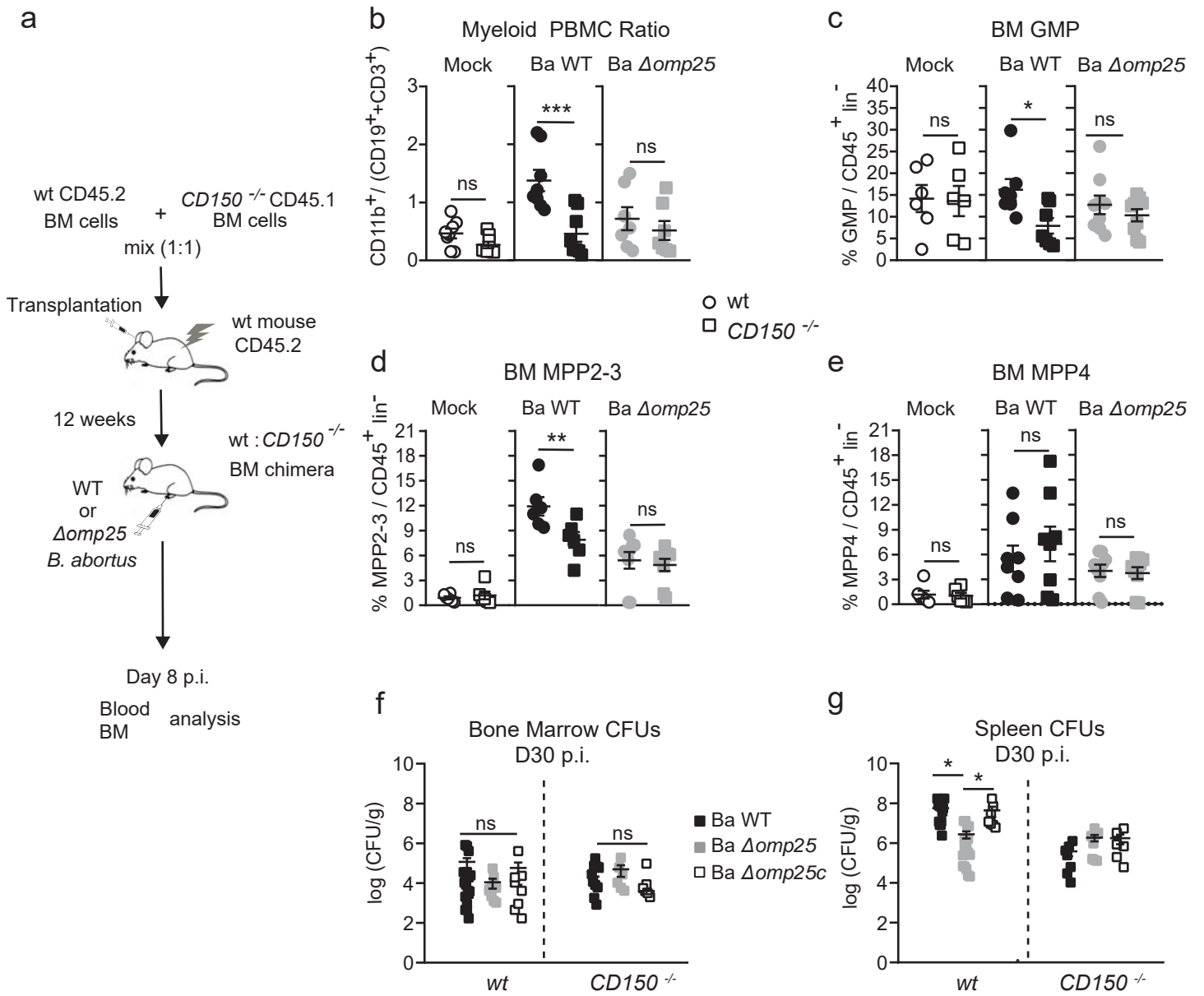
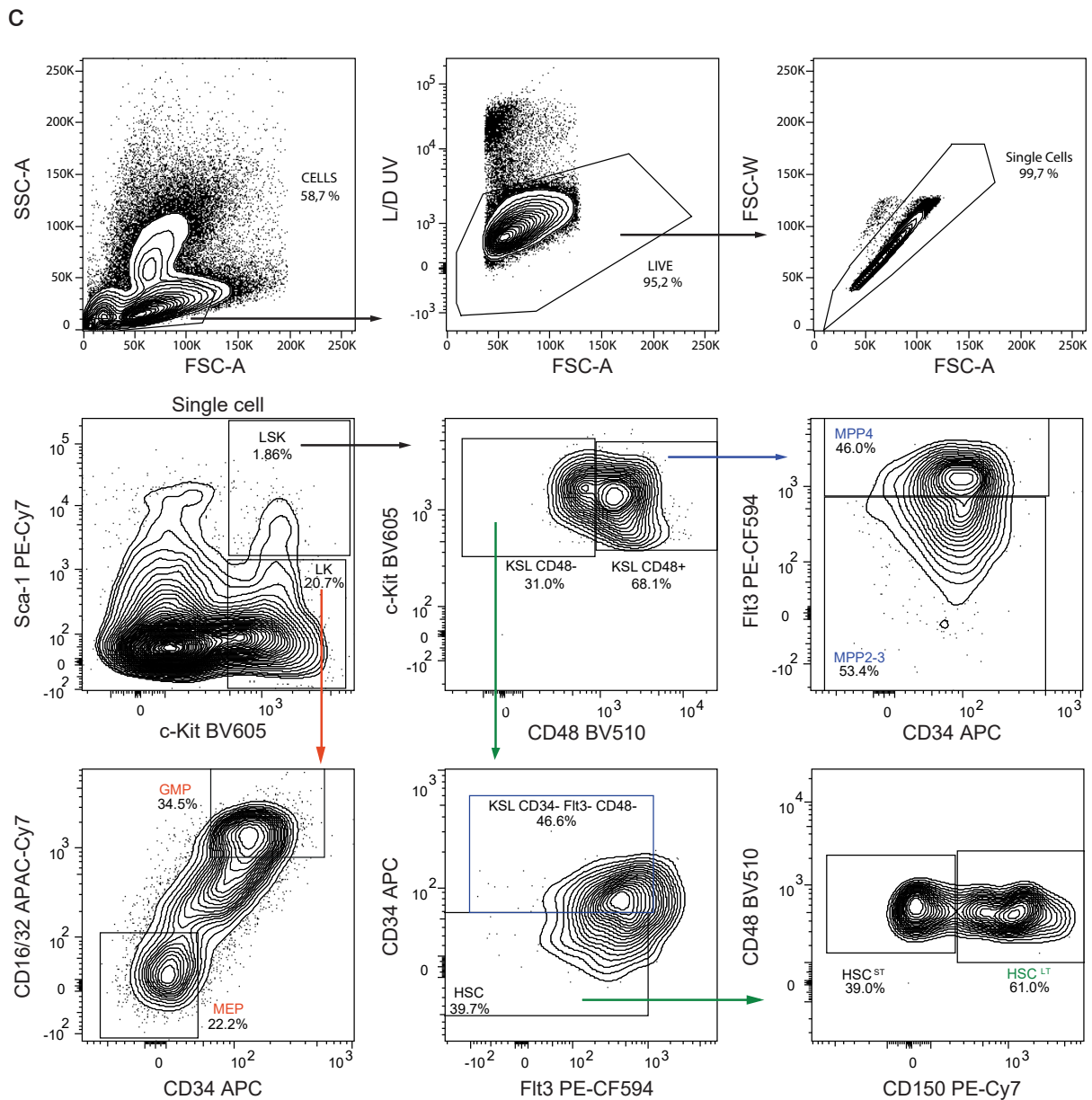
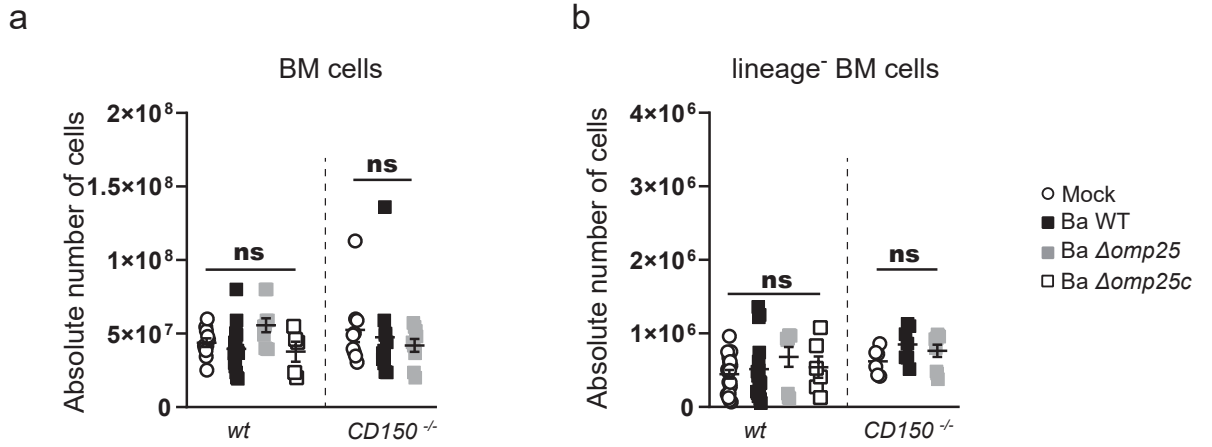
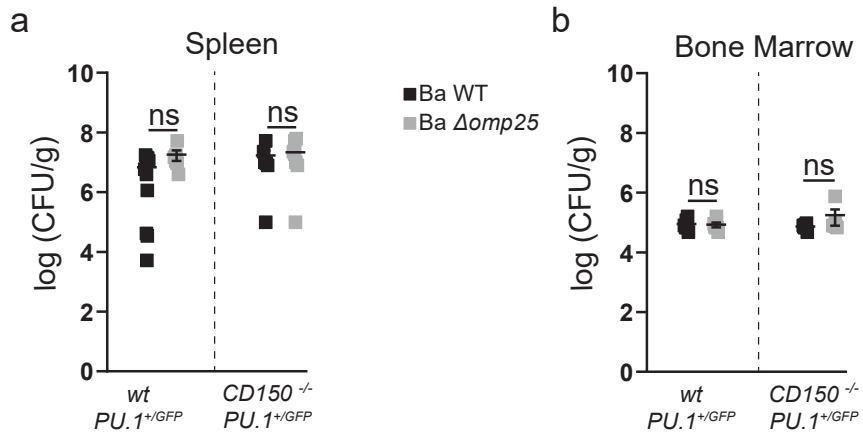


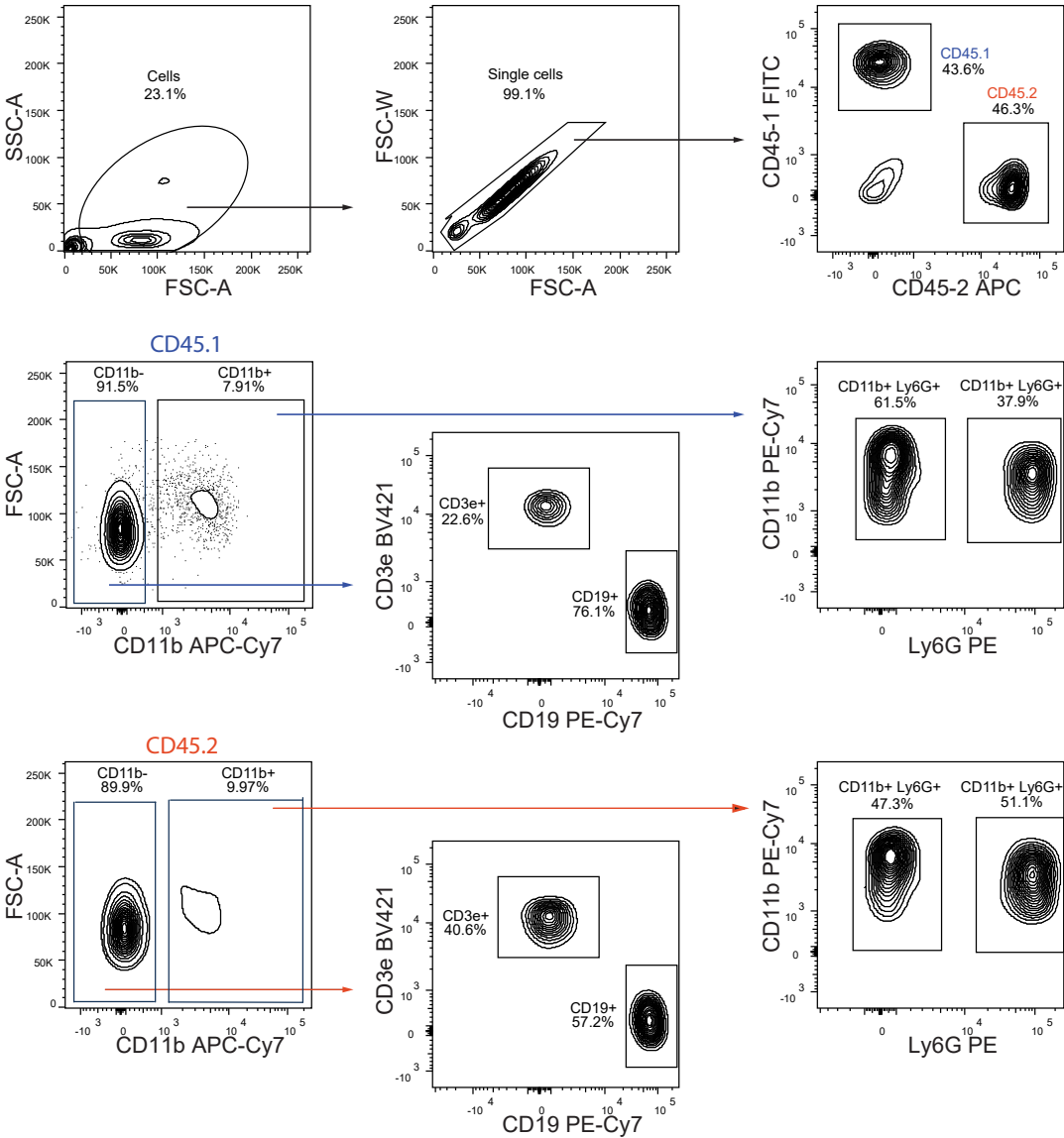
Fig.4





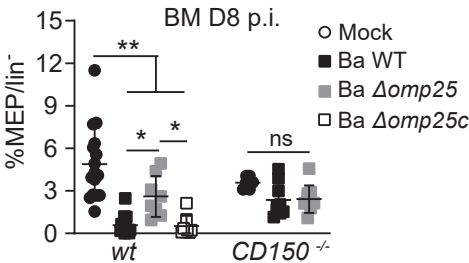


Supplementary 3

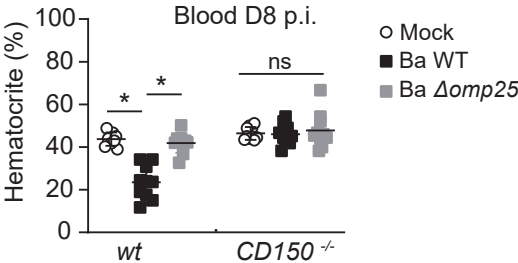


Supplementary 4

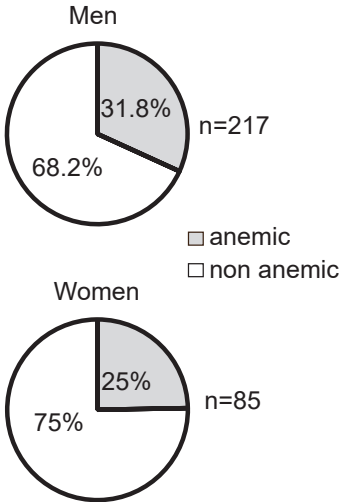
a



b



c



d

